

The Induan-Olenekian Boundary (IOB) in Mud – an update of the candidate GSSP section M04

L. Krystyn¹, S. Richoz¹ and O. N. Bhargava²

¹Department of Palaeontology – Geozentrum, A-1090 Wien, Althanstrasse 14,

leopold.krystyn@univie.ac.at

²103, Sector 7, Panchkula 134109, Haryana, India.

Abstract A refined study of the Induan–Olenekian boundary beds in Mud has evidenced differences in the boundary relevant fauna of the formerly faunistically undifferentiated bed 13A. The latter bed could be subdivided along internal partings into three sub-beds of which the lower (13A1) demonstrates a pronounced shallowing and the beginning of a prominent $\delta^{13}\text{C}$ excursion. Fragmented brachiopod shells and crinoid ossicles characterize its fossil contents, ammonoids are almost absent; conodonts occur abundantly represented by *Bo.* (=Chengyuania) *nepalensis*, *N. cristagalli* and by the appearance of *N. novaehollandiae*. Sub-bed 13A2 contains the first Olenekian-typical ammonoids including *Rohillites rohilla*, *Parahedenstroemia* and *Kashmirites*, whereas the conodont fauna is similar to 13A1 with additional entry of *N. posterolongatus* and *E. hamadei*. The 10–12 cm thick sub-bed 13A3 shows a well-preserved ammonoid fauna of the rohilla Zone and a rich conodont association of the above cited species plus first representatives of *N. waageni* s.l. According to the recommendation of the Subcommittee on Triassic Stratigraphy, the FA of *N. waageni* s.l. is used to define the IOB at the base of sub-bed 13A3 in section M04 of Mud. The boundary is located close to but distinctly above a probably wider recognizable sequence boundary between beds 12C and 13A and around a prominent positive

1. Introduction

Following a demand of some members of the IOB Task group, we present the results of a most recent (August 2007) and more detailed resampling of the proposed GSSP candidate section in Mud (Spiti Himalaya, Fig. 1). Some of the data are quite surprising and shed new light on the suitability of the proposed boundary event (FA of the conodont *Neospathodus waageni* s.l.) for an interregional and/or intercontinental correlatability of the boundary. In the following paragraphs, we will only deal with the I-O boundary relevant interval of candidate section M04 (including M04A), for a more general background the reader may refer to the earlier documentation in Krystyn et al., 2007 and Orchard et al., 2007.

Based on the presence of the above mentioned boundary-diagnostic conodonts in M04 the sequence documentation is restricted to an interval of 1 m including 2 bed bundles (12, 13) with 6 individual beds (12 A, 12 B, 12C; 13A, 13B, 13C) and 3 sub-beds in 13A and 2 in 13C (Fig. 2). New sedimentary data are presented for the mentioned interval whereas the faunistic update is concentrated on the three sub-beds of 13A and the lower half of 13B (=conodont sample 13B1). Earlier intense collection of macrofossils has produced a rather hard and fresh rock surface in M04, which hampered the extraction of new macrofauna. Fortunately, additional material from well-weathered rock could be collected along strike 70m to the west of M04 where an identical litho-sequence of slightly different thickness (called as M04A, see Fig. 4) allowed an exact bed-by-bed

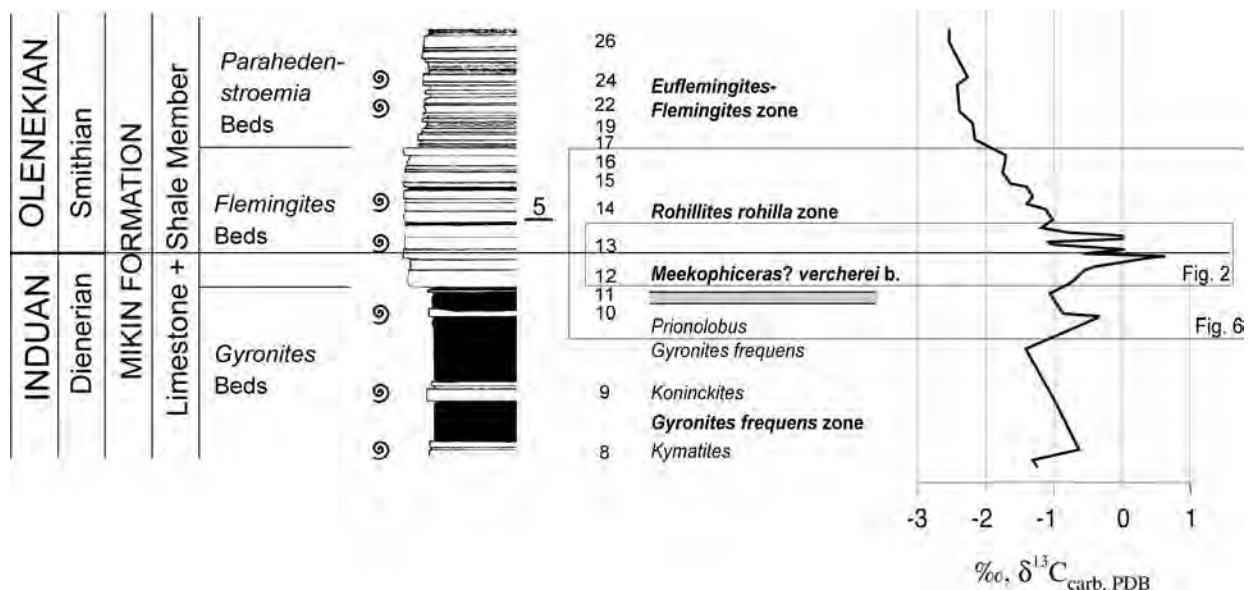


Figure 1: Lower Triassic (Induan, lower Olenekian) litho-, bio- and chemostratigraphy in Mud.

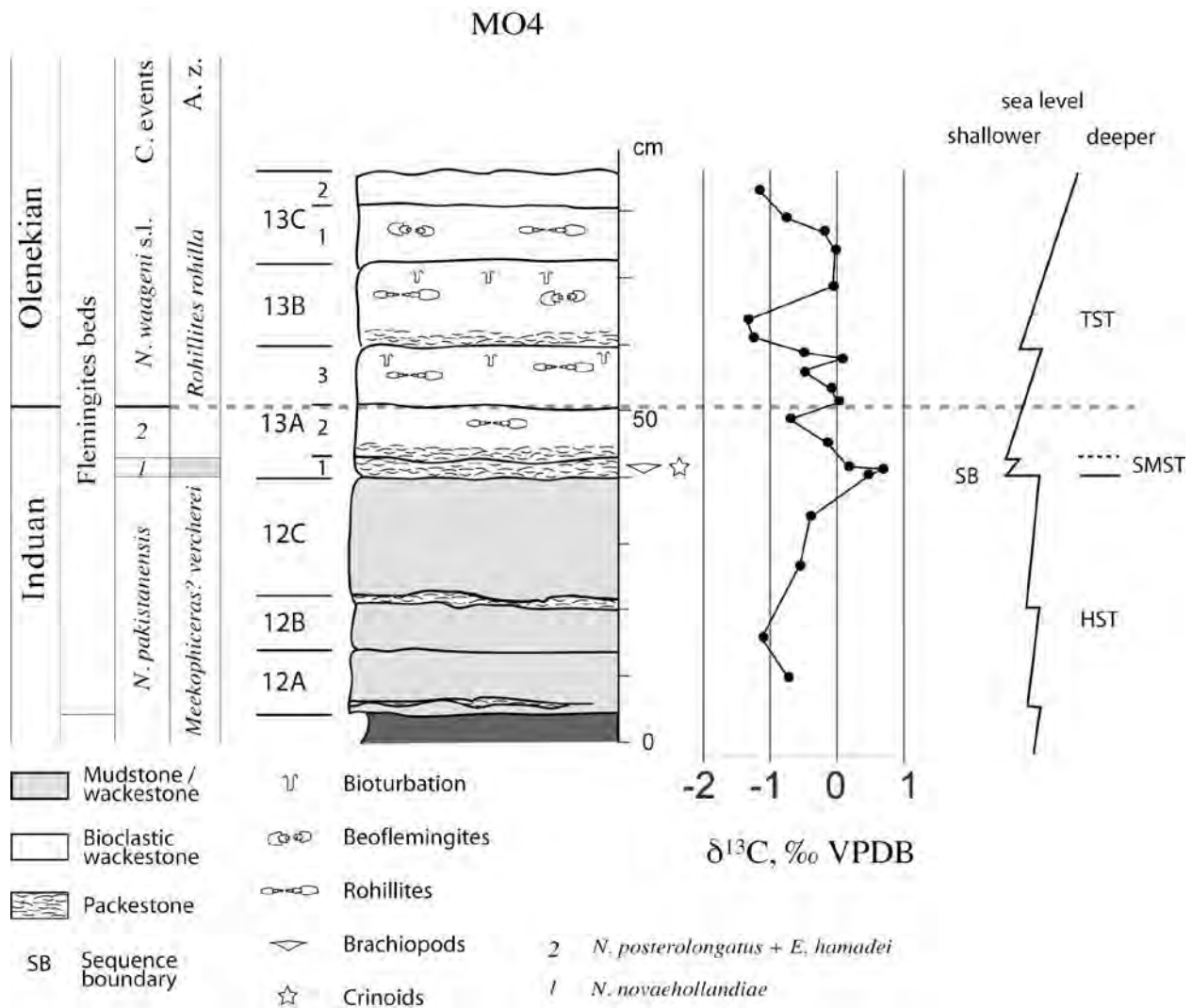


Figure 2: Detailed bedding sequence, microfacies, sequence stratigraphy, conodont and ammonoid events, sea level interpretation and carbon isotope curve in the GSSP candidate section M04.

correlation of the two sites. New cm-scaled carbon isotope data of these two sections and of a third one (M05) show mirroring high-resolution profiles and demonstrate the reliability of the earlier presented curve of section M04 (Richo et al., 2007).

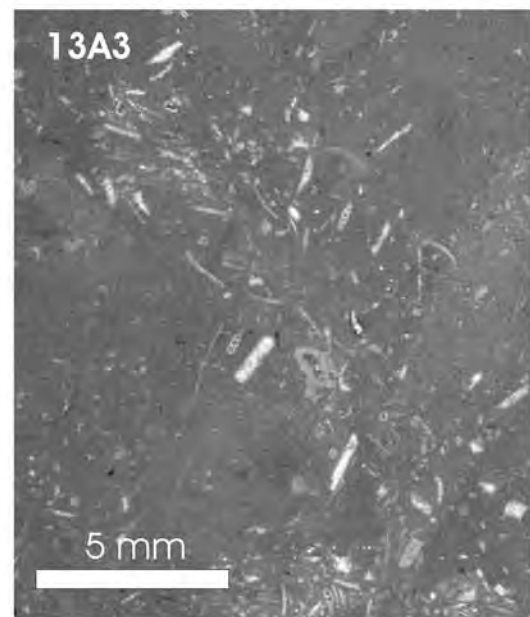
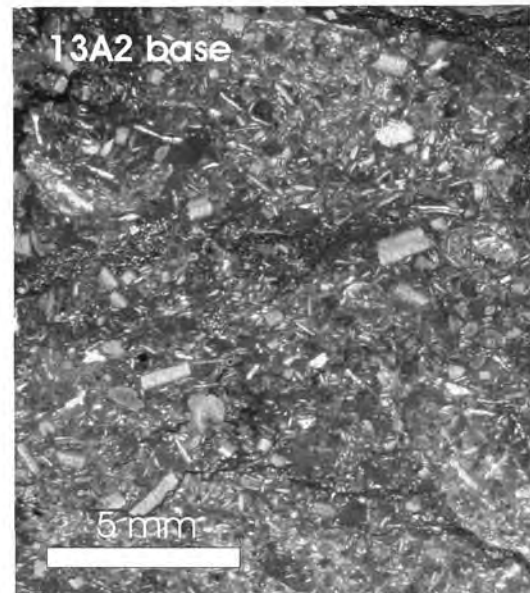
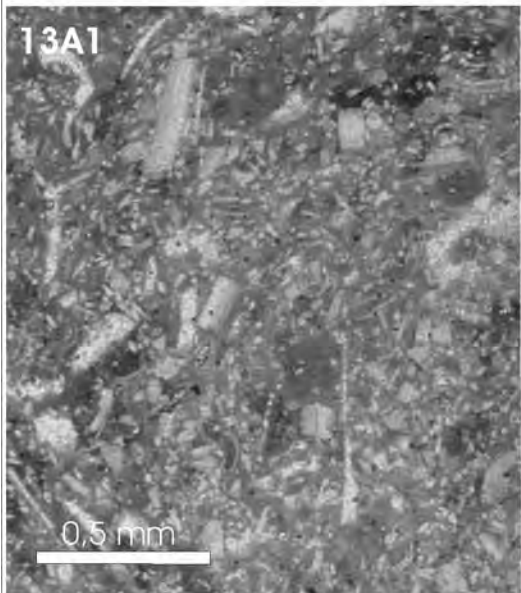
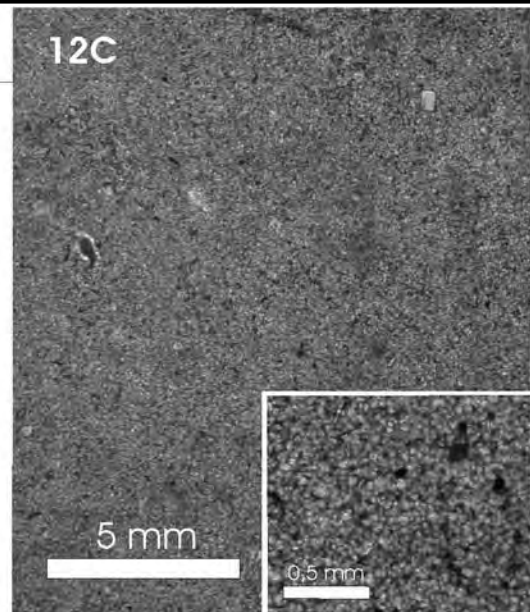
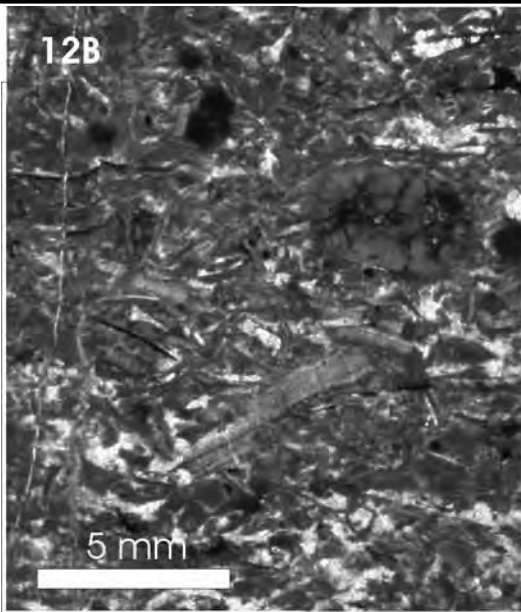
2. Sequence and depositional setting

Many beds of the Mikin Formation with some variation in thickness have been found to be continuous over an aerial distance of more than 40 km in a folded terrain. If un-folded, the distance between Losar and Mud and between Mud and Lalung will be at least 55 km and 65 km respectively. Lateral continuation of beds of even small thickness points to regular slow deposition on a wide/broad shelf of extremely gentle inclination in a period of tectonic quiescence. Presently we are concerned particularly with beds 12 and 13.

Pure grainstone layers (e.g. 12B top, Fig. 3) are restricted to interval 12, where they form sharp-based thin and discontinuous layers under- and overlain by homogeneous secondarily recrystallized mudstone (e.g. 12C, Fig. 3). The 12B shows unsorted mm-sized intraclasts and bioclasts of thin-shelled bivalves, and thicker-shelled brachiopod

fragments of probably shallower origin. It is interpreted as a storm-generated event bed made of current-induced laterally widely transported material. Coarse layers in 13A-1 (Fig. 3) and basal 13A-2 (Fig. 3) are built dominantly by bioclastic packstone with subordinate grainstone nests. They consist of densely packed small bioclasts (< 1 mm) of brachiopods, crinoids and predominantly thin-shelled molluscs. Bioturbation - recorded in common, up to 5 mm thick, burrows enriched in bioclasts - may have destroyed the primary texture (eventually graded?). The upper part of 13A-2 (Fig. 3) changes gradually to a bioclastic wackestone with loosely spaced shell fragments of pelagic bivalves, cephalopods, and rarely brachiopods. Sub-bed 13A3 is a biogen-poor wackestone (Fig. 3) with rare and small fragments of pelagic bivalves and cephalopods representing the typical Lower Triassic autochthonous deep water microfacies of Mud.

Broadly, the bedding features and the carbonate microfacies show a shoaling cycle from bed bundle 12 to sub-beds 13A-1 and 13A-2, culminating in above or close to the lower wave base that was affected by storms resulting in deposition of bioclastic pack- and grainstone layers. The litho-changes between 12C and 13A reflect a rapid change in the depositional environment from below wave



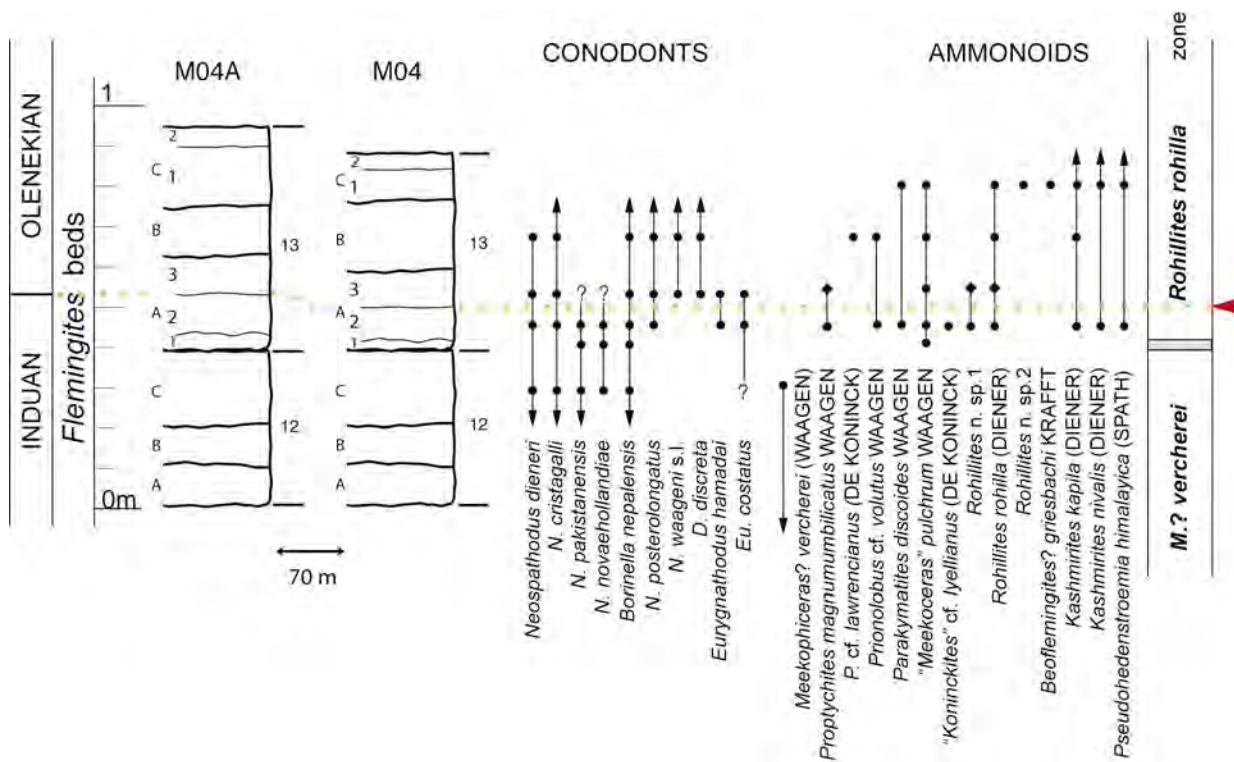


Figure 4: Vertical ranges of conodonts and ammonoids in the candidate GSSP section M04 (with additional ammonoid data from M04A, see text). Arrow marks the conodont based Induan-Olenekian boundary at the base of sub-bed 13A3.

Figure 3 (previous page): Photomicrographs of the Induan-Olenekian boundary beds of Mud M04.

12B: Grain-/packstone with unsorted mm-sized intraclasts and bioclasts of thin-shelled bivalves and thicker-shelled brachiopod fragments.

12C: Microsparite, secondarily recrystallized homogeneous mudstone.

13A1, 13A2 base: Bioclastic packstone with densely packed small bioclasts (< 1 mm) of brachiopods, crinoids and predominantly thin-shelled mollusks.

13A2: Burrowed bioclastic wackestone with loosely spaced shell fragments of pelagic bivalves, cephalopods, and rarely brachiopods.

13A3: Biogen-poor wackestone with rare and small shell fragments of pelagic bivalves and cephalopods.

base to episodic bottom-current movement and sediment winnowing due to a sea level fall. Restricted occurrence of benthonic fauna of small rhynchonellid brachiopods and crinoids also indicates shallowing and a better oxygenated bottom facies for sub-beds 13A-1 and 13A-2. The sharp C-isotope changes in MO4A and MO5 from 12C to 13A-1 could be interpreted towards a (short) break in sedimentation between bed 12 and 13 (Fig. 1). In MO4 otherwise, an initial increase of the $\delta^{13}\text{C}$ values in 12C towards the 13A-1 peak (Fig. 6) points more to stratigraphic continuity or to, if any, a non-relevant gap. This alternative is in support of a sudden change in the oceanic current system concurrent to the sea level fall and of a subsequent rapid environmental recovery with a most probably global background (Payne et al., 2004).

The following provisional sequential interpretation, subject to detailed microfacies studies, can be made: late highstand system tract (HST) in 12, lowstand system tract (LST) in 13A-1 (to eventually base of 13A-2), transgressive system

tract (TST) in 13A-2 and above [this is the text version of the initial report to the Boundary Working Group where the sea level lowstand phase at the base of 13A was called as LST. However, in exact sequence stratigraphic terminology the lowstand phase above a SB 2 has correctly to be called as SMST (shelf margin sequence tract). All previously recorded faunistic, sedimentary and facial data are in accordance with a deep marine ramp setting interpretation for the IOB in Mud (as well as the Himalayan Lower Triassic in general). The calculated water depth of at least 50-70m (i.e. below mean wave base) should therefore exclude a priori a SB 1 for which also no physical evidence (emersion, erosion, karstification, phreatic cementation) exists. The changes to bottom-winning wave activity at the base of bed 13A1 can be best interpreted as a sea level drop that, taking into account the principal flat ramp geometry of the Himalayan margin, should have affected regionally a wide area. The flat geometry should have also created wide lateral facies shifts even by minor sea level changes. The discussed results therefore point to a submarine SB 2 with continuous water depth of below 50 m in Mud].

The sequence boundary between 12 and 13, therefore, implies not necessarily a break, and if present, it should have been too short to be geologically or stratigraphically relevant. A time-corresponding sequence boundary called as “natural mid-Lower Triassic boundary” (Henderson, 2005) of large lateral extent in Western Canada could be seen as supporting the idea of a coeval worldwide sea level change useful as an additional correlation tool. Though, according to the available sequential and stratigraphic data, the sea level drop seems to have lasted only for short, it had a tremendous oceanographic and faunistic impact as manifested in the marine geochemistry and the explosive faunal radiation at the IOB.

Biostratigraphy

Conodont fauna

Mud has a much richer and more diverse conodont fauna than Chaohu. Details on the emended conodont succession of Mud are contained in the “Report on 2007 conodont collections from Mud, Spiti” by M. Orchard in this Albertiana volume. Two sets of samples (each sample weighting app. 4 kg) have been collected from M04 and M04A (Fig. 4). M. Orchard, whose results are summarized below, has studied the conodonts from M04 in Vancouver:

1) Within bed 13A three successive FO events are discriminated:

- Appearance of *Neospathodus novaehollandiae* in sub-bed 13A-1
- Appearance of *Neospathodus posterolongatus* and *Eurygnathodus hamadei* in 13A-2
- Appearance of *Neospathodus waageni* s. l. in 13A-3

2) Base of 13A3 records a frequency change from *Borinella nepalensis* to *Neospathodus posterolongatus* dominance, an abundance peak of *Eurygnathodus* and ?disappearance of *Neospathodus cristagalli*.

3) Changes in conodont fauna are gradual and specimens show no signs of corrosion or reworking; samples are very rich in individuals of all sizes.

4) Both the successive appearances of different species as well as the highly differing faunal spectra in the sub-beds of 13A are a strong argument against an interpretation of 13A as a single storm-induced event bed.

The Vienna sample set from M04A has yet to be studied in more detail but it shows a coeval appearance date of *Neospathodus waageni* s. l. in 13A3. This date seems therefore qualified to define the Induan-Olenekian boundary in section M04 at the base of sub-bed 13A3.

Absence of *N. waageni eowaageni* in Mud, in our opinion, points to a general rare and limited occurrence of this form. Looking to its record in West Pindingshan substantiates this conclusion because the FAD is based on 1 specimen in sub-bed 24-16 while the next higher and more common report is fairly above, in the *N. posterolongatus* appearance level (sub-bed 24-20) according to CTWG, 2007 (internal task force report). This underlines the accuracy of the STS decision to use the *N. waageni* s.l. date for defining the IOB.

Ammonoid fauna

The ammonoid fauna of the Olenekian base in Mud is currently worldwide unique and there is nothing in Chaohu that may be of help for a detailed correlation. The slow replacement rate of Induan taxa by Olenekian ones in the boundary beds of Mud again points to a continuous sedimentary record and against a break. The low paleolatitude and wide geographical distribution of the *Rohillites* fauna has been demonstrated by Bruewhiler et al., 2007 (Fig. 5).

Ammonoids are almost missing in sub-bed 13A1 (Fig. 4) except for a single specimen of “*Meekoceras pulchrum* Waagen (Pl. 2, fig. 4) found in M04A. *Paranorites aequalis* Spath, 1934 from the upper(?) Ceratite Marls of the Salt Range is morphologically very close and could be a younger synonym. Zhakarov (pers. comm., 2007) compares “*Meekoceras pulchrum* with *Lepiskites kolymensis* (Popov, 1961) The two forms are, however, different in body shape by the narrow, strongly tabulate venter and the smooth shell of the former (see Waagen, 1895, pl. 29, fig. 1c) and the externally rounded, well ribbed phragmocone of the latter (Dagys and Ermakova, 1990, pls. 15-17). “*Meekoceras pulchrum* (Waagen) may cross the IOB as it has originally been described from a low position in the Ceratite Marls of the Salt Range. The sub-bed 13A1 is, thus, of indistinctive zonal age.

No ammonoids could be detected and collected in 13A2 of M04 and it is, therefore, highly probable that all earlier findings from 13A do belong to 13A3. New 13A2 material comes from subsection M04A where fossils are common and the weathered rock surface allowed their extraction. Though the fauna is less well preserved than in 13A3 (no shell preservation) yet is easily determinable to species level. The new M04A collection contains several

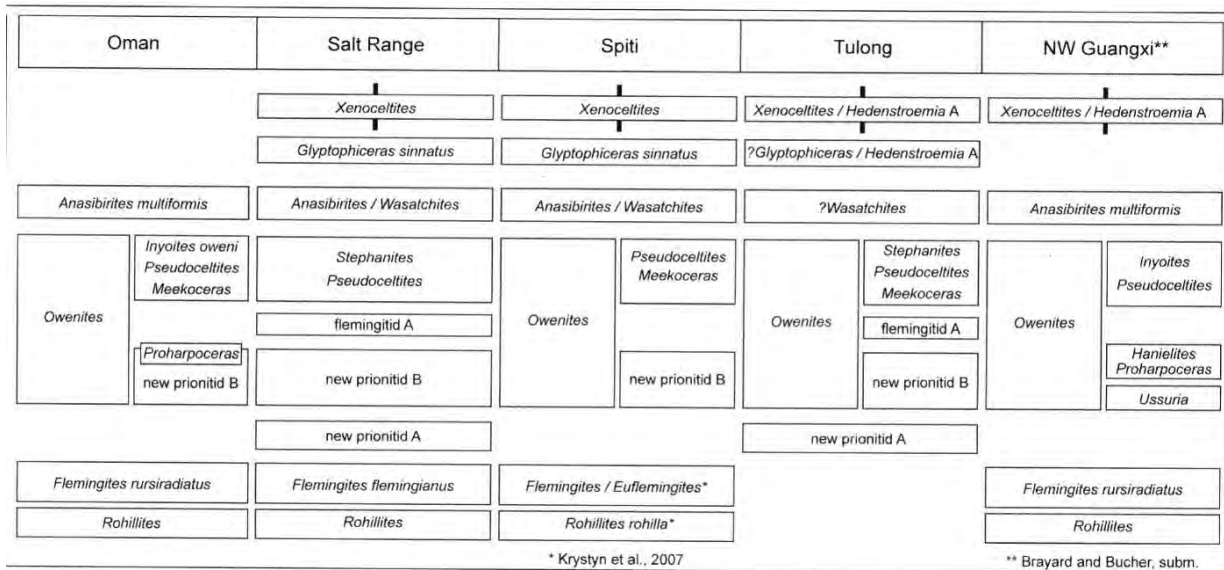


Figure 5: Correlation of Smithian Tethyan ammonoid successions (Brüwhiler et al., 2007). Note wide geographic extent of the *Rohillites* interval below the *Flemingites* zone.

specimens of “*Meekoceras*” *pulchrum* (Pl. 2, fig. 4) and *Kashmirites kapila* (Diener), and a single set of *Rohillites* n. sp. 1 (Pl. 2, fig. 2), *Rohillites rohilla* Diener, *Proptychites magnumumbilicatus* Waagen, *Prionolobus* cf. *volutus* Waagen, *Parakymatites discoides* Waagen, “*Koninckites*” *lyellianus* (De Koninck), *Parahedenstroemia himalayica* (Spath), and *Kashmirites nivalis* (Diener). Almost all these forms occur also in the undifferentiated sub-beds 13A2/3 of sections M03 to M06 (plates 1 and 2).

The ammonoid fauna of sub-beds 13A2 and 13A3 constitutes an interesting and, obviously, a natural melange of Induan and Olenekian taxa. Induan holdovers are *Proptychites*, *Prionolobus* and *Koninckites*, Olenekian innovations include *Rohillites*, *Parahedenstroemia* and *Pseudaspidites*. The FO of *Rohillites* in 13A2 defines currently the base of the *rohilla* Zone in Mud. Several of the above-mentioned species recur in Waagen’s upper(?) Ceratite Marls of the Salt Range and may indicate partial contemporaneity of Frech’s *Prionolobus volutus* Zone with the Himalayan *rohilla* Zone. Below the *volutus* Zone, Frech (1905) discriminated another zone based on *Celtites* (now *Bernhardites*) *radiosus*, a species, which may well belong to *Kashmirites* and if so, it would also point to an Induan onset of this genus.

Carbon isotope stratigraphy

A first detailed documentation of the $\delta^{13}C$ -curve of Mud was published by Richoz et al., (2007). This study was criticized for its synthetic curve combined from different sections, and because of some contradictory results between the sections M03 and M04. To resolve these problems, the IOB interval (Beds 12 to 14) has been resampled in detail (at least one sample each 8cm) in four different sections: M03, M04 (the proposed GSSP), M04A, 70m along the strike and M05 situated still higher up (see cover figure of Albertiana v. 35). Renewed investigation of section M03 has produced again depleted values and confirms the earlier result that these section underwent an alteration of the

primary carbon isotopic signal, eventually due to a local, bedding plane-parallel fault at the base of the *Flemingites* Beds seen only in M03. Data from M04, M04A and M05 sections show a perfect fit and correlation capacity (Fig. 6) and confirm - in more detail - the results published by Richoz et al. (2007). We see the excellent correlation between these three sections as well with Losar 60km away (Atudorei, 1999), as a confirmation of the primary origin of the isotopic signal in the proposed GSSP of Mud. The IOB peak may be worldwide identifiable and clusters in Mud around the FA of *N. waageni* s.l. in beds 13A+B.

The $\delta^{13}C$ -curve (Figs. 1, 6) fluctuates in the top-Gyronites Beds (beds 11-12) around -1‰, followed by a sharp positive excursion of 1 to 2‰ of amplitude leading to a prominent peak close to 1‰ in the base of Bed 13A (13A-1). The $\delta^{13}C$ -curve shows then a decrease of around 1.5‰ from 13A2 to the base of 13B. In the middle of bed 13B is recorded a sharp and short peak of around 1‰ amplitude. From top of 13B to 13C there is a rapid return to more negative values of around -1‰. Within bed 14 occur only minor variations till a small negative shift in 15B leads to values around -1.5‰ and then to - 2‰ in bed 17. In summary, the Mud curve is characterized by a distinct inflexion point between values increasing from the *Otoceras* beds to decreasing values till the *Parahedenstroemia* beds in connection with a well-marked positive excursion (of 2‰) in the basal *rohilla* Zone (from 13A to 13B; Fig. 1).

To avoid the problem of an over-interpretation of single data points we do not interpret not reproducible changes <1‰ value as such low differences in bulk rock samples may rely on subordinate changes in rock composition and chemistry. We have to consider that the IOB falls in a time of important oceanographic change and thus a sampling in different heights (even on cm scale) of bed 12 C can easily produce deviant signals explaining the small noticed discrepancies. The “sharp” shift between 12C and 13A with the best spatial resolution in M04 has an amplitude of 0,9‰, with 8cm between the two samples making it

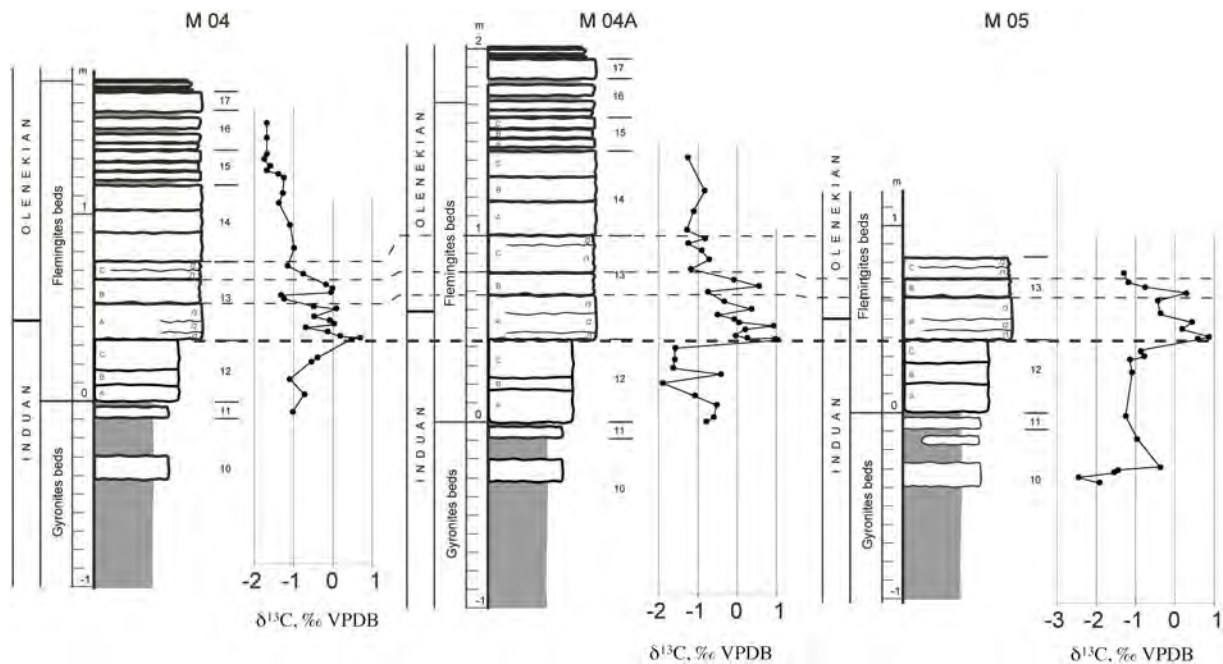


Figure 6: $\delta^{13}\text{C}$ isotope curve of the I-O boundary beds in Mud. The positive peak and inflexion point in beds 13A and 13B is a good chemostratigraphic marker for the proposed boundary. Note the distinct and widely recorded early Smithian negative trend from 13C onwards, starting above the appearance of *N. waageni*, and the high level of concordance between sections M04, M04A and M05.

insufficient to conclude a gap. West Pindingshan shows many sudden jumps of 1-2‰ between successive samples (Fig. 7, cf. CTWG, 2007, fig. 13 and 15), often stronger than in Mud. Until now nobody has concluded that each of these changes may record a gap. Certain strongly deviant values are especially developed within bed 25 in WP and, if isolated considered, may lead to serious misinterpretations (Korte et al., 2007 – Horacek, pers. comm.).

There is now common agreement that this IOB sharp and strong positive carbon isotope excursion (CIE) reflects a primary and drastic change in ocean circulation (Payne et al., 2004, 2007; Corsetti et al., 2005, Richoz 2006, Zuo et al., 2006; Richoz et al., 2007, Horacek et al., 2007 (a,b,c), Galfetti et al., 2007, Tong et al., 2007). We have marked in figure 7 with a red (in black & white grey) bar the full width of the positive excursion with an amplitude greater than 1‰ around the IOB. This excursion is in Mud and West Pindingshan too small to be one by one compared with the 3-7‰ excursion amplitudes of many other (mostly shallow water) sections. The CIE is equally short-lived in all three measured sections of Mud. In terms of bio-events it starts slightly below the FA of *N. waageni* s.l. and ends soon above this date (Fig. 7) representing a short time space of less than half of one *short* ammonoid zone (*rohilla* Z.). The two figured West Pindingshan CIEs (Fig. 7) otherwise are both much wider and show different ranges based on an additional marked negative excursion in the CWTG 2007, fig. 15 curve beginning below the FA of *N. waageni* s.l. and ending after the FO of *N. waageni waageni*. This leads to the image that the Horacek et al., (2007c) CIE is starting early in the Induan whereas the CWTG, 2007 CIE follows later slightly above *N. waageni* s.l. Noteworthy is that both CIE end well above the FA of *N. spitiensis* and thereby distinctly (one ammonoid zone,

Flemingites-Euflemingites Z.) later than in Mud and in North Pingdingshan (CTWG, 2007). The in shape and time deviating WP curve(s) demonstrate in this comparison the current problem in Chaohu to use the isotopic signal as a *high-resolution* event marker.

To use a CIE as a globally instantaneous event means first to test its supposed isochrony against an accurate high-resolution biozonal scheme. This fine-tuned scale is presently from no other sections than Chaohu and Mud available. It is therefore unjustified and scientifically unsound from our current regional chronostratigraphic database to declare single points of the IOB-CIE as reference for specific biotic events. Proposing exactly this, Korte et al. (2007, p.4) declare: "Mud would be the only locality in the world where the maximum in $\delta^{13}\text{C}$ lie before the base of the Olenekian", which is unsubstantiated and objectively wrong. A careful biostratigraphic evaluation of their cited sections leads to a contrasting result: in Iran, Italy (Horacek et al., 2007a,b) and Turkey (Richoz, 2006) the IOB is placed primarily on the CIE, without any *waageni* control. In Pufels, (N Italy), the only place with own marine bio-data, Korte et al., (2005) define the base of the Smithian on the FAD of *Pachycladina obliqua*, a shallow-water conodont of reduced biostratigraphic correlation potential whose FO dates to the Dienerian. In Wadi Maqam, Oman, Richoz (2006) shows the first appearance of *N. waageni* contemporary to the isotope peak but without additional bio-data from below, and with sparse isotopic data. Several biostratigraphically better constrained isotope curves are known from China, where in Guizhou Payne et al., (2004) place the CIE clearly below the FO of *N. waageni* and of *Platyvillosus* (= *Eurygnathodus*); in Meishan, Guandao and Zuodeng, the positive peak is also below the IOB, in Hushan, Daxiakou und Lekang, it is slightly above (Tong

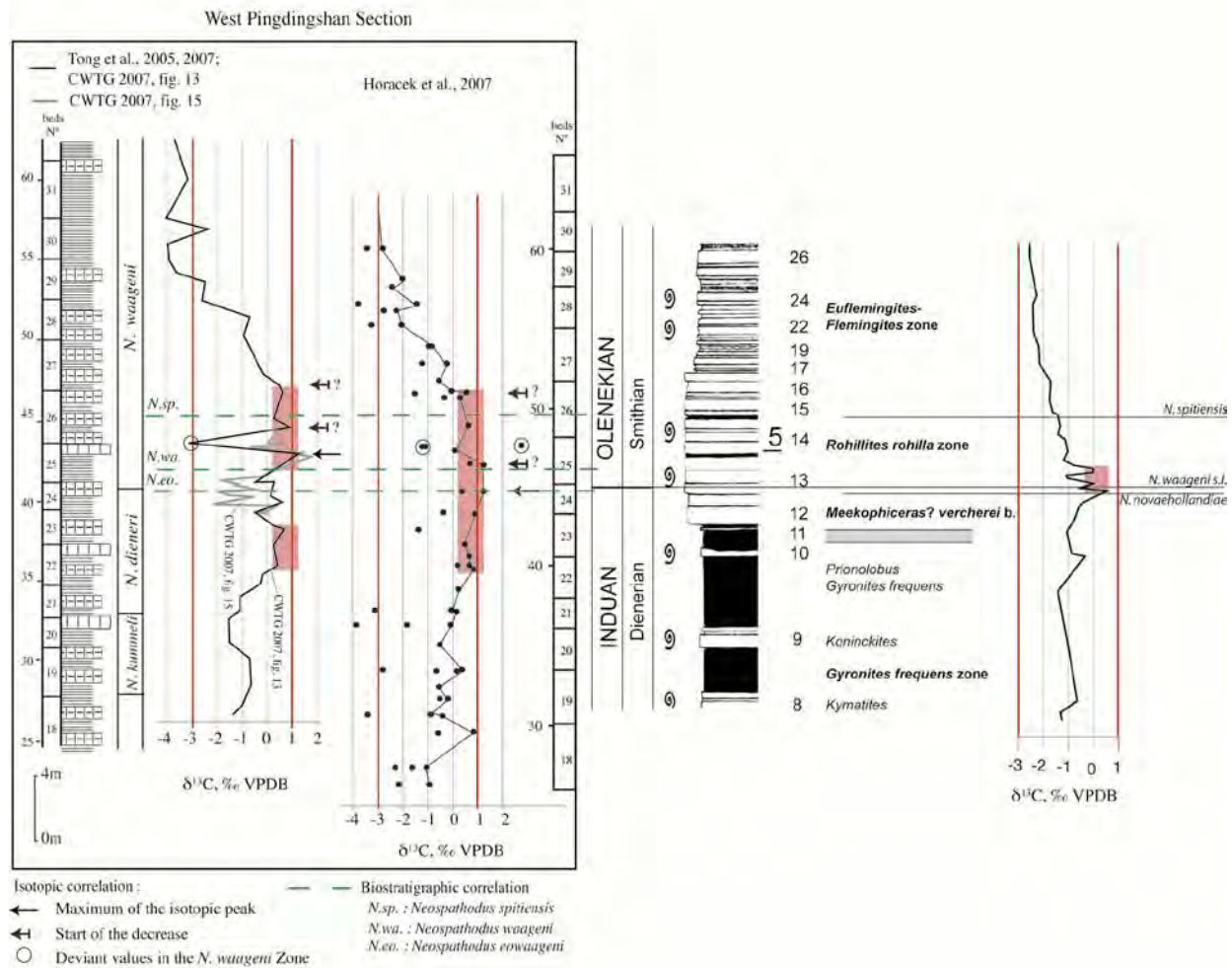


Figure 7: Comparison of the $\delta^{13}\text{C}$ isotope curve of the I-O boundary interval in Mud and West Pingdingshan (CTWG, 2007 and Horacek et al. 2007c). The red (in black & white grey) bar marks the full width of the positive excursion around the IOB with an amplitude greater than 1‰.

et al., 2007); in NW Guangxi, Galfetti et al., 2007 show the CIE within the *Kashmirites* beds (counterpart of the *rohilla* Z.) what could correspond to a position below, together with or above the *waageni* date; and only in West and North Pingdingshan (version in CTWG, 2007), the peak is clearly above – but for West Pingdingshan, the position of the peak above FO of *N. waageni* is not so clear in the dataset of Horacek et al. (2007c), as discussed above. In summary, the evaluation of all these data results in the same conclusion drawn further up from the Mud curve: a prominent positive CIE occurs in the vicinity of the FA of *N. waageni* s.l. and, with adequate representation, can serve in fossil-poor sections as close proxy for the IOB.

Meanwhile nitrogen and organic carbon isotope as well as major, minor and trace elements analyses have also been carried out in Mud with good results (data in process of publication - Algeo, oral comm.). The Mud section is thus suitable for further chemostratigraphic studies.

Chronologic calibration of the IO boundary beds in Mud

New high-precision U-Pb ages from the biochronologically well dated Lower Triassic on NW Guangxi, China

(Galfetti et al., 2007) allow a rather exact time calculation of the Smithian ammonoid (resp. conodont) zones in Mud and West Pingdingshan. Galfetti et al., (2007) report a U-Pb age of 251,22±0,20 Ma (Chin 40) for the basal Smithian *Kashmirites densistriatus* beds of NW Guangxi, which are time-correlative to the *Rohillites rohilla* Zone in Mud (Brühwiler et al., 2007; Fig. 5). Another U-Pb date (Chin 10) of 250,55±0,40 Ma is recorded by Ovtcharova et al. (2006) for the lower Spathian *Tirolites/Columbites* beds of NW Guangxi, a time interval occurring already above the first Spathian ammonoid zone. From these data it can be safely concluded that the Smithian stage is bracketed between 0,7 and max. 1,3 Ma (Galfetti et al., 2007). Calculated durations of Smithian biochrons by cross-plotting the new U-Pb ages against sediment accumulation rates demonstrate a high level of timely coincidence between Mud and Chaohu but also extremely disproportionate zonal durations (Fig. 8). This new age constrain confirms the extremely short duration of the basal Olenekian ammonoid (*rohilla* Z.) and conodont (FA *N. waageni* s.l. – FA *N. spitiensis*) intervals and the high rate of the pelagic faunal diversification during the earliest Smithian. It further provides a more precise timing of the carbon cycle perturbations around the CIE, which according to data in

time interval	Mud MO4			Chaohu, WP		
	thickness m	time duration min max		thickness m	time duration min max	
Smithian	10,0	0,7 Ma	1,3 Ma	52,0	0,7 Ma	1,3 Ma
	5,2	0,36 Ma	0,68 Ma	27,2	0,36 Ma	0,68 Ma
<i>Flemingites- Euflemingites Zone</i>	4,0	0,28 Ma	0,52 Ma	21,2	0,28 Ma	0,52 Ma
FAD <i>waageni</i> s.l.- FAD <i>spitiensis</i> I.Z.	0,7	49 Ka	91 Ka	3,6	48,5 Ka	91 Ka
<i>rohilla</i> Z.	0,8	56 Ka	104 Ka			
CIE : Mud WP	0,4	28 Ka	52 Ka	3,0	40 Ka	75 Ka

Figure 8: Calculated durations of biochrons in Mud M04 and Chaohu (West Pindingshan) based on sediment accumulation rates versus Smithian U-Pb ages of Galfetti et al. (2007).

Fig. 8 last considerable longer in W.P. than in Mud.

Acknowledgements

This is a contribution to IGCP Project 467 (Triassic Time). LK was financially supported by the Austrian National Committee for IGCP and SR by a grant from the Swiss National Science Foundation (N° PBLA2-109819). We are most indebted to D.M. Banerjee (Delhi University) for his interest and logistic support of our work in Spiti. Special thanks are to M. Maslo for long-time help in the field. Photographic plates have been prepared by R. Gold and graphics by M. Maslo.

References

- Atudorei, N.V. 1999. Constraints on the Upper Permian to Upper Triassic marine carbon isotope curve. Case studies from the Tethys. Unpubl. PhD Thesis, Lausanne, 160pp.
- Brühwiler, T., Bucher, H., Goudemand, N. and Brayard, A., 2007. Smithian (early Triassic) ammonoid succession of the Tethys: New preliminary results from Tibet, India, Pakistan and Oman. *New Mexico Museum of Natural History and Science, Bulletin* 41, 25-26.
- Corsetti, F.A., Baud, A., Marengo, P.J., Richoz, S., 2005. Summary of Early Triassic carbon isotope records. *C.R. Palevol.* 4, 405–418.
- Dagys, A.S., and Ermakova, S.P. 1990. Early Olenekian ammonoids of Siberia. *Nauka, Moscow*, 112pp.
- Frech, F. 1905. Die Dyas: Lethaea geognostica. Theil II, Das Mesozoicum, 1. Band Trias, zweite Lieferung : Die asiatische Trias von Fritz Noetling, p. 107–221. Pl. I-XXII
- Galfetti, T., Bucher, H., Ovtcharova, M., Schaltegger, U., Brayard, A., Brühwiler, T., Goudemand, N., Weissert, H., Hochuli, P. A., Cordey, F. and Guodun, K. 2007. Timing of the Early Triassic carbon cycle perturbations inferred from new U-Pb ages and ammonoid biochronozones. *Earth and Planetary Science Letters*, 258: 593-604.
- Henderson, C. M. 2005. International correlation of the marine Permian time scale. In: Lucas, S. G. & Ziegler, K. E. (eds) *The Nonmarine Permian*, New Mexico Museum of Natural History and Science Bulletin, 30: 104–105.
- Horacek M., Brandner R, Abart R. 2007a. Carbon isotope record of the P/T boundary and the Lower Triassic in the Southern Alps: Evidence for rapid changes in storage of organic carbon. *Palaeogeography, Palaeoclimatology, Palaeoecology*, 252: 347-354.
- Horacek M., Richoz, S., Brandner, R., Krystyn, L., Spötl, C. 2007b. Evidence for recurrent changes in Lower Triassic oceanic circulation of the Tethys: The $\delta^{13}C$ record from marine sections in Iran. *Paleogeography, Paleoclimatology, Paleocology*, 252: 355-369.
- Horacek, M., Wang, X., Grossman E. L., Richoz, S., Cao Z. 2007c. The carbon-isotope curve from the Chaohu section, China: different trends at the Induan –Olenekian Boundary or diagenesis? *Albertiana*, V.35, p. 41-45.
- Korte, C., Kozur, H.W., Veizer, J., 2005, ^{13}C and ^{18}O values of Triassic brachiopods and carbonate rocks as proxies for coeval seawater and palaeotemperature: *Palaeogeography, Palaeoclimatology, Palaeoecology*, v. 226, p. 287–306.
- Korte, C., Kozur, H.W. and Bachmann, G.H., (2007) - Carbon isotope values of Triassic lacustrine and hypersaline playa-lake carbonates: Lower Buntsandstein and Middle Keuper (Germany). *Hallesches Jahrb. Geowiss.* V. 29, p. 1 – 10.
- Krystyn, L., Bhargava, O.N. and Richoz, R. 2007. A candidate GSSP for the base of the Olenekian stage: Mud at Pin Valley; district Lahul & Spiti, Himachal Pradesh (Western Himalaya), India. *Albertiana*, 35: 5-29.
- Orchard, M.J. and Krystyn, L. 2007. Conodonts from the Induan-Olenekian boundary interval at Mud, Spiti. *Albertiana*, 35: 30-34.
- Ovtcharova, M., Bucher, H., Schaltegger, U., Galfetti, T., Brayard, A., Guex, J. 2006 New biochronozones and implications for the timing of the Triassic biotic recovery: *Earth Planet. Sci. Lett.* 243, p. 463–475.
- Payne, J. L., Lehrmann, D. J., Wei, J. Y., Orchard, M. J., Schrag, D. P., Knoll, A. H. 2004. Large Perturbations

- of the Carbon Cycle During Recovery from the End-Permian Extinction, *Science*, 305: 506-509.
- Payne, J.L. & Kump, L.R., 2007, Evidence for recurrent Early Triassic massive volcanism from quantitative interpretation of carbon isotope fluctuations, *Earth and Planetary Science Letters*, V 256 (1-2), p. 264-277.
- Richoz, S., 2006. Stratigraphie et variations isotopiques du carbone dans le Permien supérieur et le Trias inférieur de la Néotéthys (Turquie, Oman et Iran). *Mémoires de Géologie (Lausanne)*, 46, 275 p.
- Richoz, S., Krystyn, L., Horacek, M. and Spötl, C. 2007. Carbon isotope record of the Induan-Olenekian candidate GSSP Mud and comparison with other sections. *Albertiana*, 35: 35-40.
- Tong J. Zuo, J., Chen Z.Q. 2007. Early Triassic carbon isotope excursions from South china: Proxies for devastation and restoration of marine ecosystems following the end-Permian mass extinction. *Geological Journal* 42: 371-389.
- Waagen, W. 1895. Fossils from the Ceratite Formation. *Pal. Indica* (13), Salt Range Fossils V. II : 1-323, pl. I-XL.
- Zuo, J., Tong, J., Qiu, H. & Zhao, L. 2006. Carbon isotope composition of the Lower Triassic marine carbonates, Lower Yangtze Region, South China. *Science in China: Serie D Earth Sciences*, 49(3): 225-241.

Specimens are figured in natural size and housed in the collection of the Department of Palaeontology, Vienna University.

Plate 1

Fig. 1: *Meekophiceras? vercherei* (Waagen); M03-12B

Fig. 2: *Rohillites rohilla* (Diener); M04-13A-2/3

Plate 1



1a



1b



2

Plate 2

Fig. 1: *Rohillites* n. sp. 1; M06-13A2/3

Fig. 2: *Rohillites* n. sp. 1; M04A-13A2

Fig. 3: *Rohillites rohilla* (Diener); M04-13C

Fig. 4: “*Meekoceras*” *pulchrum* Waagen; M04-13A1

Fig. 5: “*Meekoceras*” *pulchrum* Waagen; M04-13B

